A Appendix / supplemental material
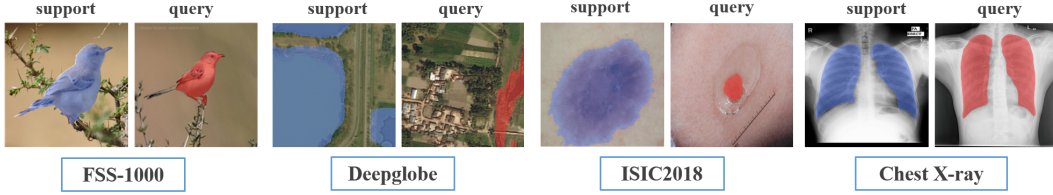
A.1 More Dataset Details

Figure 7: Examples of segmentation for four target datasets.

Our experimental setup is grounded in the benchmark established by PATNet [24]. Fig. 7 presents an example of segmentation for four target datasets. Further details follow:

PASCAL-5^i [35] extends the PASCAL VOC 2012 [13] by integrating additional annotations from the SDS dataset [17]. Utilizing PASCAL-5^i as our source domain for training, we then evaluate the models' performance across four target datasets.

FSS-1000 [26] is a few-shot segmentation dataset comprising 1000 natural image categories, with each category containing 10 samples. In our experiment, we adhere to the official split for semantic segmentation and report results on the designated testing set, which encompasses 240 classes and 2,400 images. We consider FSS-1000 as our designated target domain for testing.

Deepglobe [10] consists of satellite images annotated densely at the pixel level across 7 categories: urban, agriculture, rangeland, forest, water, barren, and unknown. Since ground-truth labels are available only in the training set, we utilize the official training dataset comprising 803 images to showcase our results. We designate it as our testing target domain and follow the same processing approach as PATNet.

ISIC2018 [9, 38] is designed specifically for skin cancer screening and comprises images of lesions, with each image depicting exactly one primary lesion. Adhering to the guidelines established by PATNet, we process and utilize the dataset, considering ISIC2018 as our target domain for testing.

Chest X-ray [6, 20] is tailored for Tuberculosis diagnosis, comprising 566 images with a resolution of 4020×4892 pixels. These images depict cases from 58 Tuberculosis patients and 80 individuals with normal conditions. A common approach to handling large image sizes involves resizing them to 1024×1024 pixels.

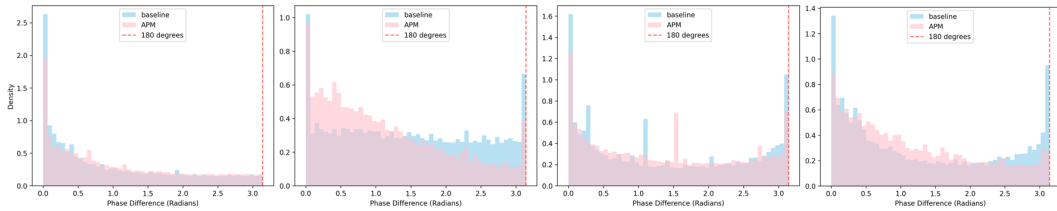## A.2 APM Reduces Inter-Channel Correlation by Frequency Domain Mask

Figure 8: Histogram of phase differences (weighted by amplitude) between channels in the feature maps before and after APM.

As shown in Figure 8, we present histograms of the phase differences between channels in the feature maps (weighted by amplitude) before and after adding the APM module. After applying APM, the phase differences between channels concentrated around 0 and π are reduced, which aligns with our mathematical derivation in the main text. The APM decreases the correlation between feature map channels by altering phase and amplitude, thereby enhancing the independence of their semantic representations. Additionally, due to the use of finer-grained frequency domain partitioning, APM performs well on FSS-1000 compared to the simple high-low frequency partitioning at the input level.
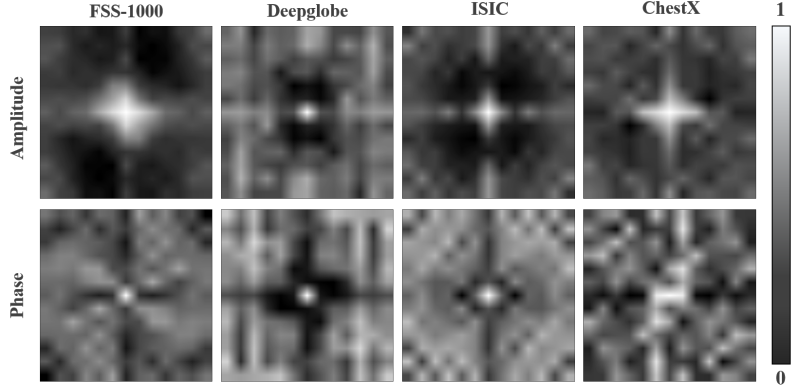
Figure 9: The visualization of the frequency components filtered by the masker.

A.3 Analyze the Frequency Components Filtered by the APM

The visualization results in Figure 9 show the average frequency components filtered by the amplitude masker and phase masker across different domains. The center represents low frequencies, while the periphery represents high frequencies. White indicates a value of 1, meaning the frequency component passes through, and black indicates a value of 0, meaning the frequency component is filtered out. For FSS, the amplitude masker (AM) primarily filters out mid-to-high-frequency components, while the phase masker (PM) mainly retains mid-frequency components. For DeepGlobe, both AM and PM retain more mid-to-high frequencies. For ISIC, AM filters out more mid-to-high frequencies, retaining low frequencies, whereas PM retains relatively more mid frequencies. For ChestX, AM mainly retains low-frequency components, while PM filters out frequencies across the spectrum, retaining relatively more low-to-mid frequencies. These results align well with the patterns observed in Figure 1 of our main text. It is evident that for different targets, AM and PM dynamically and adaptively filter different frequency components, selecting those more beneficial for the current domain. Additionally, the advantageous amplitude and phase frequency components vary across different target domains, underscoring the necessity of considering amplitude and phase separately.

A.4 Detailed Ablation Study Results

In the main text, we demonstrate the effectiveness of our various designs by presenting the average mIoU. Here, as shown in Table 10, we provide detailed results on each target dataset.

Table 10: Detailed ablation study results of various designs (Backbone: ResNet-50).

APM-S	APM-M	ACPA	FSS-1000		Deepglobe		ISIC		Chest X-ray		Average	
			1-shot	5-shot	1-shot	5-shot	1-shot	5-shot	1-shot	5-shot	1-shot	5-shot
			77.54	80.21	33.19	36.46	32.65	35.09	47.34	48.63	47.68	50.10
✓			77.98	79.85	40.74	44.80	38.79	44.16	73.55	76.73	57.77	61.39
✓		✓	78.25	80.29	40.77	44.85	41.48	49.39	75.22	76.89	58.93	62.86
	✓		78.98	81.21	40.81	44.82	38.99	45.49	77.73	82.60	59.13	63.53
	✓	✓	79.29	81.83	40.86	44.92	41.71	51.16	78.25	82.81	60.03	65.18

A.5 Broader Impact

Our research delves into the phenomenon that filtering specific frequency components based on different domains significantly improves performance, providing an interpretation. Furthermore, we demonstrated the relationship between frequency components and inter-channel correlation through mathematical derivation. Building on our interpretation and derivation, we propose the APM, a feature-level frequency component mask designed to enhance the generalization of feature map representations. Further, we introduced Adaptive Channel Phase Attention (ACPA). Based on the APM-optimized feature map, the ACPA encourages the model to focus on more effective features while aligning the feature spaces of the support and query. Experimental results demonstrate the effectiveness of our approach significantly enhances the model's cross-domain transferability. This work is applicable not only to CDFSS but also to other areas like domain generalization and domain adaptation. Future research will aim to broaden our evaluations to encompass a wider range of target domains, enhancing our understanding of their performance in various real-world scenarios.